

## Mutations in *WNT7A* Cause a Range of Limb Malformations, Including Fuhrmann Syndrome and Al-Awadi/Raas-Rothschild/Schinzel Phocomelia Syndrome

C. G. Woods,\* S. Stricker,\* P. Seemann, R. Stern, J. Cox, E. Sherridan, E. Roberts, K. Springell, S. Scott, G. Karbani, S. M. Sharif, C. Toomes, J. Bond, D. Kumar, L. Al-Gazali, and S. Mundlos

Fuhrmann syndrome and the Al-Awadi/Raas-Rothschild/Schinzel phocomelia syndrome are considered to be distinct limb-malformation disorders characterized by various degrees of limb aplasia/hypoplasia and joint dysplasia in humans. In families with these syndromes, we found homozygous missense mutations in the dorsoventral-patterning gene *WNT7A* and confirmed their functional significance in retroviral-mediated transfection of chicken mesenchyme cell cultures and developing limbs. The results suggest that a partial loss of *WNT7A* function causes Fuhrmann syndrome (and a phenotype similar to mouse *Wnt7a* knockout), whereas the more-severe limb truncation phenotypes observed in Al-Awadi/Raas-Rothschild/Schinzel phocomelia syndrome result from null mutations (and cause a phenotype similar to mouse *Shh* knockout). These findings illustrate the specific and conserved importance of *WNT7A* in multiple aspects of vertebrate limb development.

The tetrapod limb develops as an outgrowth of mesenchymal cells, from the lateral plate mesoderm, that are covered by a layer of ectoderm. Over time, the limb bud grows and lengthens, giving rise to the various components of the limb: skeleton, muscles, tendons, and nerves. The limb skeleton is laid down progressively, starting with the most proximal part—that is, humerus/femur—and finishing with the most distal, the tips of finger and toes. This complex patterning process is determined by a three-dimensional signaling system that defines a proximodistal axis (from shoulder to finger tip), an anteroposterior axis (from radius/thumb to the ulna/little finger), and a dorsoventral axis (from the dorsum of the hand to the palm).

Recent studies have unraveled the major molecular components that coordinate limb outgrowth along these three axes.<sup>1</sup> The proximodistal axis is under the control of fibroblast growth factors (FGFs) from the apical ectodermal ridge (AER). The anteroposterior axis is under the control of sonic hedgehog (*SHH*) from the posterior mesenchyme (zone of polarizing activity [ZPA]), whereas the dorsoventral axis is controlled by bone morphogenetic proteins (BMPs) and engrailed (*EN1*) from the ventral ectoderm and by *Wnt7a* from the dorsal ectoderm. Traditionally, these signals are regarded as independent entities, but their activities cannot be separated, because they are mutually dependent. For example, AER and ZPA signals each induce expression of the other and the removal of one equally results in down-regulation of the other.<sup>2,3</sup> Likewise, re-

moval of the dorsal ectoderm or its signal *Wnt7a* results in a severe reduction of *SHH* expression,<sup>4,5</sup> indicating that maintenance of *SHH* expression requires both the dorsal ectoderm and the AER.

Alterations in the composition of this system—either by targeted gene inactivation in the mouse, by overexpression of certain genes in chick embryos, or by deleterious gene mutations in humans—result in specific and characteristic phenotypes.<sup>6,7</sup> Inactivation of *Wnt7a* in mouse, for example, results in a loss of dorsal structures of the distal limb that manifests as bivalent autopods with footpads on both sides.<sup>4</sup> *Wnt7a* defines the dorsoventral axis by inducing the expression of the transcription factor *Lmx1* in the dorsal mesenchyme of the developing limb.<sup>8</sup> Mutations in *Lmx1*, in turn, result in nail-patella syndrome, a human condition characterized by loss of dorsal features, with nail dysplasia, hypoplastic patellae, and other skeletal changes.<sup>9</sup> The expression of *Wnt7a* is restricted to the dorsal ectoderm because it is repressed by *EN1* in the ventral ectoderm. Inactivation of *EN1* results in double-dorsal limbs, probably because of the successive misexpression of *WNT7A* in the ventral ectoderm.<sup>10</sup> We describe here the developmental defects of the human limb caused by malfunction of *WNT7A*, which were unexpectedly more severe than the mouse mutant phenotype.

**Clinical findings.**—We investigated two families with an autosomal recessive disorder that caused significant limb shortening with marked fibular and ulnar hypoplasia (fig.

From the Department of Medical Genetics, Cambridge Institute for Medical Research, University of Cambridge, Cambridge, United Kingdom (C.G.W.; R.S.; J.C.); Max-Planck Institute for Molecular Genetics and Institute for Medical Genetics, Charité, Berlin (S. Stricker; P.S.; S.M.); Department of Clinical Genetics (E.S.; G.K.; S.M.S.) and Section of Ophthalmology and Neuroscience, Leeds Institute of Molecular Medicine (E.R.; K.S.; S. Scott; C.T.; J.B.), St James's University Hospital, Leeds, United Kingdom; Centre for Human Genetics, Sheffield Children's Hospital, Sheffield, United Kingdom (D.K.); and Department of Paediatrics, Faculty of Medicine and Health Sciences, United Arab Emirates University, Al-Anin, United Arab Emirates (L.A.-G.)

Received March 29, 2006; accepted for publication May 30, 2006; electronically published June 23, 2006.

Address for correspondence and reprints: Dr. C. G. Woods, Department of Medical Genetics, Cambridge Institute for Medical Research, University of Cambridge, Hills Road, Cambridge CB2 2XY, United Kingdom. E-mail: cw347@cam.ac.uk

\* These two authors contributed equally to this work.

Am. J. Hum. Genet. 2006;79:402–408. © 2006 by The American Society of Human Genetics. All rights reserved. 0002-9297/2006/7902-0025\$15.00

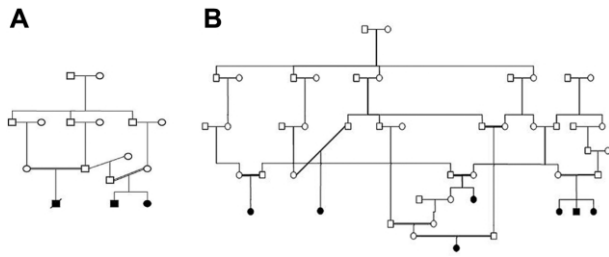


**Figure 1.** Pedigrees of families with Fuhrmann and Al-Awadi/Raas-Rothschild/Schinzel phocomelia syndrome. *A*, Family 1, in which affected individuals received the diagnosis of “absence of ulnar and fibula with severe limb deficiency” (Al-Awadi/Raas-Rothschild/Schinzel phocomelia syndrome). *B*, Family 2, in which affected individuals received the diagnosis of “fibular aplasia or hypoplasia, femoral bowing, and poly-, syn-, and oligodactyly (Fuhrmann syndrome).”

1A and 1B). Family 1 had three affected children (figs. 1A and 2), whose diagnosis was “absence of ulnar and fibula with severe limb deficiency” (MIM 276820, also known as “Al-Awadi/Raas-Rothschild syndrome, Schinzel phocomelia syndrome, and limb/pelvis-hypoplasia/aplasia syndrome.” The first child exhibited ectrodactyly of the right hand, with nail dysplasia; contractures at the right elbow joint; no left elbow joint, with the left arm ending with an appendage that looked like a deformed finger with dysplastic nail; lower limbs replaced by a stick-like appendage (more severe on the right side). The second child had complete absence of the lower limbs, and both upper limbs lacked an elbow joint and ended with a deformed finger-like appendage with dysplastic nails. Both children had normal intelligence and health.

The phenotype of family 2 is described and illustrated in detail elsewhere<sup>14</sup>; two further affected individuals were born, subsequent to that publication, who conform to the original phenotype (fig. 1B). In the upper limbs, hypoplasia/aplasia of the ulnar rays was identified, which was accompanied by shortening and bowing of the radius. The fifth digits were hypoplastic, but all other elements were present. There was hypoplasia of the nails, with a radial-ulnar gradient, and the thumbs were most severely affected, with complete absence of nails. The dorsal side of the hands showed an abnormal texture, with hypoplastic flexion creases. The pelvis was highly abnormal, with hypoplastic iliac wings and, in one case, absent os ischii. The proximal ends of the femura were fully dislocated and medially bent. The patellae were absent, and, in one subject, the knee joints were fused. There was complete absence of the toenails and loss of individual toes. The degree to which individuals were affected varied within the family; however, per-person limb involvement was symmetrical, legs were more affected than arms, and the functional deficit was far greater than that expected because of limb shortening alone. The females who have passed

through puberty have not had menses. However, neither endocrine studies nor ultrasound examinations to detect malformations of the internal genitalia have been performed. Given the interindividual variability within the family, the diagnosis was, in most cases, “fibular aplasia or hypoplasia, femoral bowing and poly-, syn-, and oligodactyly” (MIM 228930) (originally known as “Fuhrmann syndrome”).

**Molecular genetics.**—We linked both families to a 2.5-Mb/4-cM region of chromosome 3p25.1 bounded by SNPs *rs1021679* and *rs3846122* (summarized in fig. 3A). Initially, DNA from three individuals from family 1 was amplified and hybridized to Affymetrix 10K SNP chips. The experimental output was analyzed by the ExcludeAR program.<sup>15</sup> This indicated a single homozygous concordant region of nine SNPs spanning 3 cM, which we confirmed in all affected members of both families by use of polymorphic microsatellite markers (data not shown). Within this region, *WNT7A* was a candidate gene because of its known involvement in limb development<sup>4,8</sup> (Wnt Web site). We designed primers for all exons and splice sites of *WNT7A*, we sequenced genomic DNA from affected members of both families (fig. 3B) using Human Genome

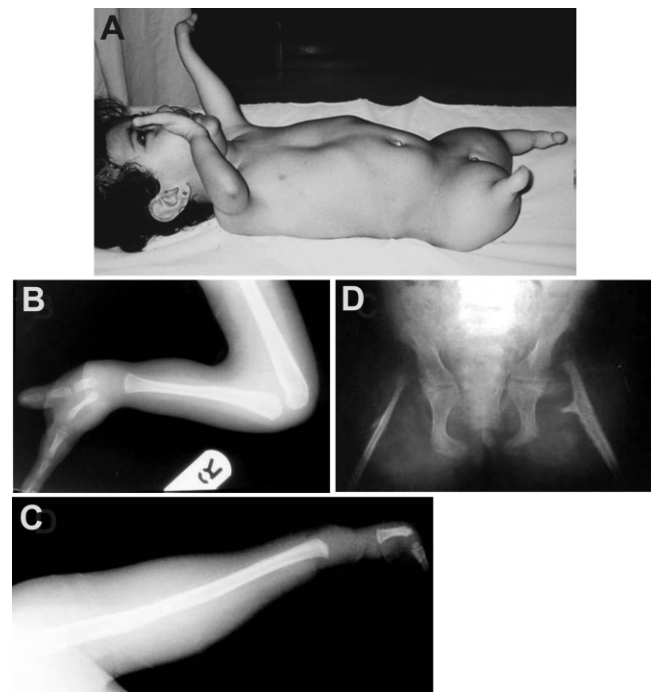


**Figure 2.** Clinical and radiographic features of an affected child from family 1. *A*, Overview of an affected female child, showing gross lower- and severe upper-limb anomalies. *B*, The child’s right arm, showing absent ulnar bone, three missing fingers on the ulnar side, and no carpals. *C*, X-ray of the child’s left limb, showing a single arm bone, absent carpal bones, and a thumb-like terminal appendage. *D*, X-ray of the child’s pelvis and lower-limb remnants. Note severe hip dysplasia and femur hypoplasia.

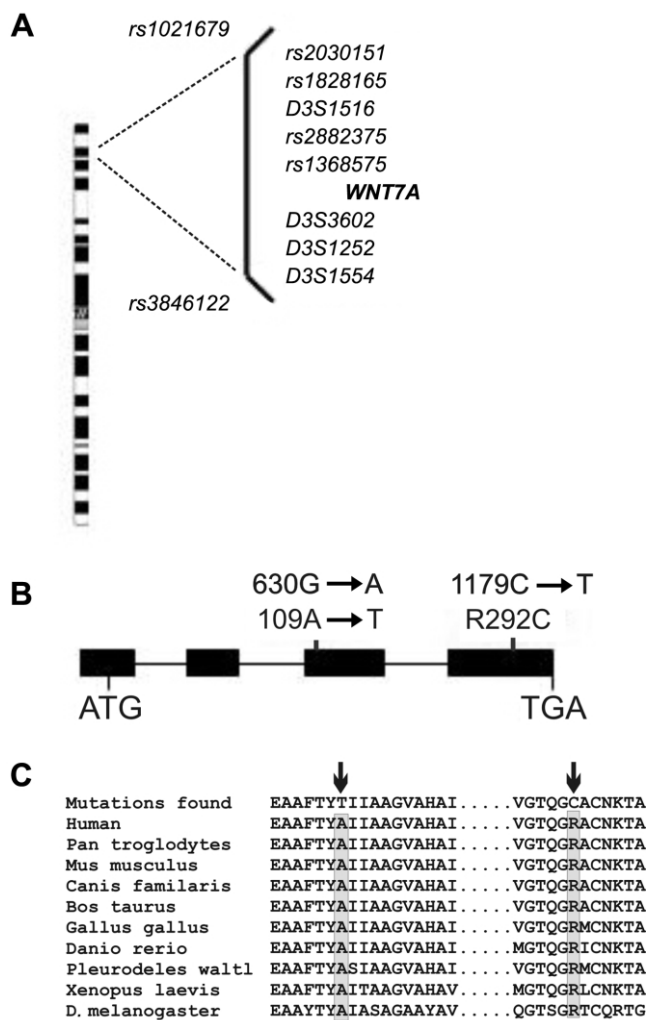


**Figure 3.** Results of molecular genetic studies that determined that mutations in *WNT7A* cause Fuhrmann syndrome and Al-Awadi/Raas-Rothschild/Schinzel phocomelia syndrome. *A*, Chromosome 3, with the region of linkage to 3p25.1 expanded to show the markers homozygous in all affected family members (*right of the bar*) and heterozygous SNPs defining the extent of the linked region (*left of the bar*). The position of *WNT7A* is shown relative to the markers. *B*, *WNT7A* exon structure, with the start and stop codons identified. The two homozygous mutations found in the present study are shown. *C*, Protein sequence surrounding the *WNT7A* mutations found in this study, aligned with *Wnt7a* sequence from other species. The alanine altered in A109T and the arginine altered in R292C are invariant and are shaded gray. The sequence of the *Drosophila melanogaster* DWnt2, the orthologue of mammalian *Wnt7a*, is shown: the two equivalent amino acids are also conserved.

Browser and Primer3, and we checked for specificity using BLAST. Mutation screening was performed by direct bidirectional sequencing of genomic DNA with use of standard methods. Primer sequences are available from the authors. In family 1, we identified a single homozygous missense mutation in exon 4, 1179C→T, that led to an arginine→cysteine substitution (R292C). In family 2, we

found three homozygous changes, all in exon 3: a missense mutation, 630G→A, that led to an alanine→threonine substitution (A109T) and two known synonymous SNPs, rs3762719 and rs12639607. The mutations were confirmed: 630G→A by ARMS and 1179C→T by exon amplification followed by *Bst*UI restriction-enzyme digestion. Both missense mutations segregated correctly within the respective families. The mutations were not present in 300 control chromosomes and were not previously described in public domain DNA databases. Both mutations led to changes of invariant amino acids in the *WNT7A* protein (fig. 3C).

*Chicken developmental studies.*—We assessed the functional significance of the two missense mutations in vivo and in vitro models of limb development and chondrocyte differentiation, respectively (summarized in fig. 4). Replication competent avian sarcoma (RCAS) retroviral vector carrying the coding sequence of mouse *Wnt7a* was a kind gift from Cliff Tabin. Site-directed mutagenesis was performed with the QuikChange Kit (Stratagene). Viral supernatants were produced and concentrated as described elsewhere.<sup>11</sup> Chick limb micromass cultures were used as an in vitro bioassay to test for *Wnt7a* wild-type and mutant activity, since it was reported elsewhere that *Wnt7a* is able to interfere with cartilage condensation in this experimental setup.<sup>16</sup> Cultures were generated from early-stage mesenchymal limb-bud cells seeded at high density,<sup>13</sup> to allow their spontaneous differentiation into chondrocytes and the formation of cartilage, which occurs in nodules that can be visualized by staining with Alcian blue and/or alkaline phosphatase (ALP) (fig. 4A). For each condition, four replicates were infected with 1  $\mu$ l concentrated viral supernatant of *Wnt7a*, A109T, or R292C. The enhanced green fluorescent protein (EGFP)-expressing virus served as a control. The area of positively stained cells was quantified using histomorphometry and the Axio-Vision software tool AutMess (Zeiss). The infection of micromass cultures with wild-type *Wnt7a*-expressing virus resulted in an almost-complete suppression of cartilage formation, as shown by the lack of dark blue-stained nodules, and ALP activity (fig. 4B and 4C). Testing of the two mutations A109T and R292C each revealed a distinct pattern for each mutation. To confirm these results, viral supernatant was produced in two independent preparations. Concentrated viral supernatants were assayed for titer of infectious units (IU) as described elsewhere.<sup>12</sup> Titers of all preparations were comparable and had a range of 5–8  $\times 10^8$  IU/ml. Expression of the A109T virus repressed nodule formation (Alcian blue staining) to a level similar to that observed for wild-type *Wnt7a*. However, repression of nodule formation was much less efficient during infection of cells with the R292C virus (fig. 4B). When we tested for ALP activity, the A109T mutant was also more efficient than the R292C variant but significantly less efficient than wild-type *Wnt7a* (fig. 4C). In comparison with uninfected controls, infection with the R292C mutant nevertheless resulted in a significant reduction of nodule formation

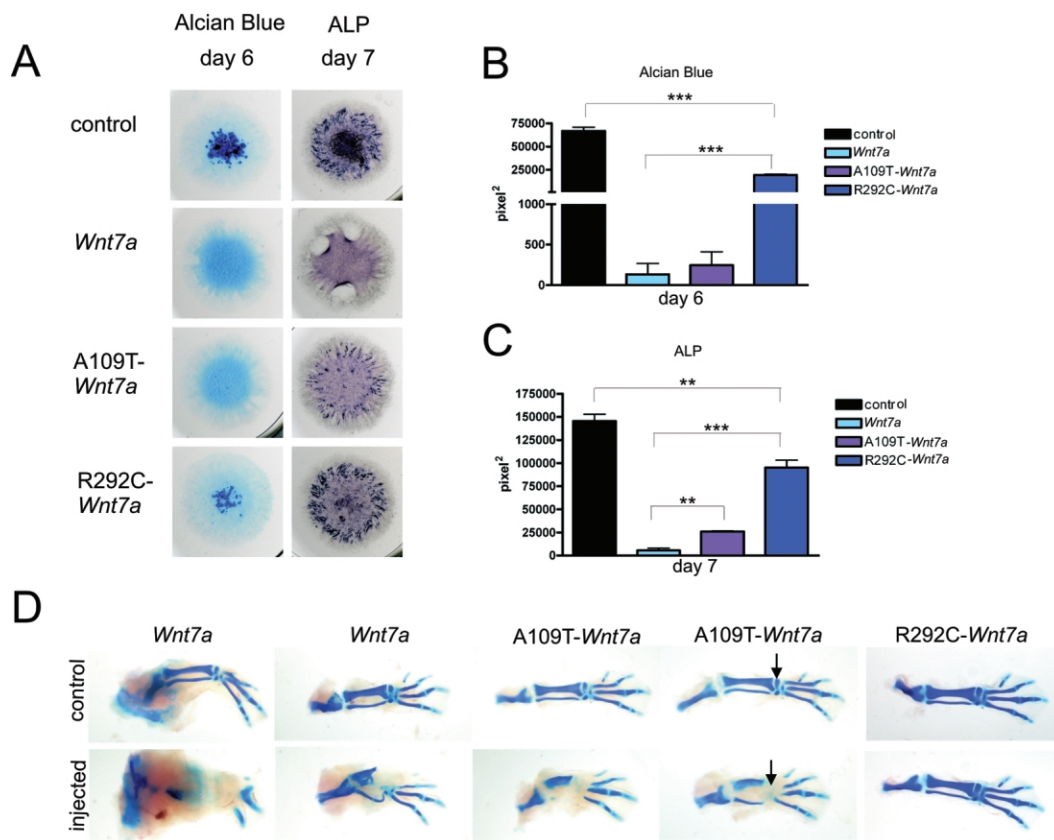


**Figure 4.** Overexpression of wild-type *WNT7A* and *WNT7A* mutants in micromass cultures and chicken hindlimbs. *A*, Photographs from micromass cultures infected with indicated constructs, after 6 d in culture (stained with Alcian blue) and after 7 d in culture (stained for ALP activity). Wild-type *WNT7A* overexpression causes a strong inhibition of chondrogenesis, as indicated by the loss of Alcian blue staining (dark blue–stained cell aggregates); the repression of ALP activity (dark brown–stained cell aggregates); and the tendency to detach from the culture dish. Overexpression of *WNT7A* mutants resulted in a reduced inhibition of chondrogenesis compared with wild-type *WNT7A*. Detachment from the culture dish was significantly delayed. *B*, Quantification of nodule formation by measurement of Alcian blue–stained surface area. Overexpression of wild-type *WNT7A* and A109T-*WNT7A* suppress the formation of nodules, whereas cells infected with R292C-*WNT7A* are able to generate nodules, albeit at a significantly reduced level. *C*, Quantification of ALP by measurement of stained surface area. Both mutants, A109T-*WNT7A* and R292C-*WNT7A*, show significantly more ALP activity than wild-type *WNT7A* but less than uninfected control cultures. *D*, Alcian blue–stained skeletal preparations of chicken hindlimbs. The upper panel shows uninfected left hindlimb (control), and the lower panel demonstrates the effects of an overexpression of the indicated constructs in the right hindlimb. Wild-type *WNT7A* overexpression resulted in severe interference with limb patterning and cartilage formation. Phenotypes varied from almost-complete lack of limb cartilage elements to hypoplasia/aplasia of single elements, mostly in the zeugopod. Overexpression of A109T-*WNT7A* generally resulted in a milder phenotype. Hypoplasia of carpals was observed in most cases; in some specimens, the tibia was absent. Overexpression of R292C-*WNT7A* had no effect on limb development, which shows that this mutation ablated *WNT7A* activity in this experimental setting.

and ALP activity. Thus, the R292C mutation results in a loss of function with some residual activity, whereas the A109T mutation retains activity that is significant but not comparable to wild-type activity (fig. 4A–4D). No difference was observed between uninfected cultures and cultures infected with an EGFP-expressing RCAS virus.

Next, we injected RCAS virus with wild-type and mutant *Wnt7a* into the right hindlimb field of chick embryos (stage HH10), as described elsewhere,<sup>12</sup> to test their activity in vivo. Embryos were harvested at stages HH32–HH35 and were stained with Alcian blue to visualize cartilage. Injection of wild-type *Wnt7a* resulted in reproducibly se-

vere phenotypes, ranging from an almost-complete loss of all skeletal elements to a partial loss affecting mainly the tibia. Infection with the A109T mutation resulted in a much less severe phenotype, with hypoplasia/aplasia of carpal anlagen as the most consistent finding. However, total absence of the fibula was also observed (fig. 4D). In contrast, infection with the R292C mutant had no effect, which indicates that this mutation was a functional null in this experimental setting.

Our in vivo and in vitro studies correlate well with the human clinical findings that the R292C mutation had a greater effect on limb morphology than did the A109T

mutation. Furthermore, our expression studies in chicken confirm the validity of this model system for the analysis of normal and abnormal limb development<sup>7</sup> and extend previous *Wnt7a* findings.<sup>5,17,18</sup> *Wnt7a* belongs to a large family of secreted signaling proteins that consists of two major functional groups: the *Wnt1* class and the *Wnt5a* class. According to the current signaling model, binding of Wnts to the Frizzled, Lrp, and/or other receptors causes a stabilization of intracellular  $\beta$ -catenin, which is then translocated into the nucleus, where it interacts with the transcription factors Lef1 and Tcf to regulate gene expression. Dependent on the receptor specificity, this pathway can be modulated by the immediate cytosolic component of the Wnt signal, Dishevelled (Dsh), which can act as a switch to reduce  $\beta$ -catenin regulation and to regulate Jun N-terminal kinase regulation. The diverse functions of Wnts during limb development are likely to be transmitted through a modulation of these pathways. For example, FGF expression in the AER can be induced by overexpression of *Wnt3a* or  $\beta$ -catenin but not by *Wnt7a*. On the other hand, only *WNT7A* and not  $\beta$ -catenin can induce *Lmx1*.<sup>19</sup> Thus, AER formation and dorsoventral polarity are controlled through distinct  $\beta$ -catenin-dependent and -independent pathways, the latter induced by *Wnt7a*. Our *in vivo* overexpression experiments showed no alteration of dorsoventral polarity, but they did show a strong repression of cartilage formation, which suggests that *Wnt7a* has a negative influence on chondrogenesis. This is in accordance with previous studies, which showed that overexpression of *Wnt7a* in ventral ectoderm is able to induce the expression of *Lmx1* but does not lead to perturbations of dorsoventral patterning of limb-cartilage elements.<sup>20</sup> Thus, overexpression of *Wnt7a* in the chick embryo cannot serve as a model for *Wnt7a* function during limb patterning. Our intention was to use this model as a bioassay to test the functional significance of the identified mutations.

Previous studies have shown that *Wnt7a* misexpression inhibits chondrogenesis *in vitro*, whereas other Wnts, such as *Wnt5a*, do not.<sup>14</sup> It has been suggested that this inhibition is due to an up-regulation of N-cadherin expression, an important mediator of cell adhesion.<sup>17</sup> The process of condensation during chondrogenesis *in vivo* or the formation of nodules in our *in vitro* system requires a down-regulation of cell adhesion. Our results are in agreement with these findings, since prolonged incubation (>7 d) of wild-type *Wnt7a*-infected cells invariably resulted in a peeling of cells from the surface, a strong indication of altered adhesion properties. This phenomenon was rarely observed in cultures infected with the mutant versions of *Wnt7a*, which indicates a loss of function. In another assay, the A109T mutant retained most of its activity and was still able to suppress formation of cartilage, similar to wild-type *Wnt7a*. However, the analysis of ALP activity makes a partial loss of function apparent, which is even more obvious in the *in vivo* experiments, where this mu-

tant was clearly less efficient than the wild type. The R292C mutant, in contrast, has retained some repressive activity *in vitro* but has no effect *in vivo*, a finding that correlates well with the much more severe phenotype in the patients with this mutation.

We have identified a range of limb hypodysplasias that are caused by mutation in *WNT7A*, including the Fuhrmann syndrome and the Al-Awadi/Raas-Rothschild and Schinzel phocomelia syndromes described elsewhere. The latter are considered the same clinical entity yet are distinct from Fuhrmann syndrome, although there is feature overlap. In family 2 (with the A109T mutation), the defect consists of ulnar/fibular ray malformations, whereas, in family 1 (with the R292C mutation), a severe truncation phenotype with aplasia/hypoplasia of distal structures is apparent. Affected individuals from both families show hypoplasia of the nails and absent patellae, as seen in nail-patella syndrome due to *LMX1* mutations. These structures are under control of dorsal specification and thus *Wnt7a*. The phenotype in family 2 is similar to that in mice with inactivated *Wnt7a* alleles.<sup>4</sup> These mice show ventralized limbs, with foot pads on both the ventral and dorsal sides of the autopod. Pigmented skin pads, which probably represent duplications of the large pads found at the distal ends of the digits, cover the rudimentary nails. In addition, loss of the ulna and of digit 5 is observed. Nail hypoplasia, as observed in the affected individuals described here, can be considered characteristic for dorsal-specification defects, since these structures are determined by signals from the dorsal ectoderm. The extreme bowing of the femur as well as the partial hypoplasia of the pelvis are not part of the mouse phenotype and support a specific role of *WNT7A* during human limb development.

The phenotype in family 1 is much more severe than in family 2. Affected individuals in family 1 show a severe distal hypoplasia with joint fusions. The remaining distal structures consist of single bones that have completely lost their polarity. The loss of anterior/posterior patterning is demonstrated by the presence of a single bone replacing the radius/ulna and the hand on one side, whereas the missing dorsal/ventral pattern is exposed by the lack of nails or any other dorsal structures. In the lower extremities, the changes are even more severe, resulting in complete truncations distal of a rudimentary femur-like structure. This degree of malformation is not observed in mice with inactivated *Wnt7a* alleles.<sup>4,21</sup> Instead, mice with inactivated *Shh* appear to have a phenotype very similar to that of the patients described here: truncation of hindlimbs and replacement of radius/ulna by a single skeletal element that is fused with the humerus.<sup>22,23</sup> Furthermore, limb truncations are observed in individuals with acheiro-podia, a condition caused by deletions within the *LMBR1* gene, which is likely to contain regulatory sequences for *SHH*.<sup>6,23</sup> *Wnt7a* is expressed in the flanking ectoderm of the trunk prior to limb-bud outgrowth and thus prior to *SHH* expression. Studies in mice with inactivated *Wnt7a*

alleles have shown that *Shh* is initially expressed in the absence of *Wnt7a*. However, a day later in development, the number of *Shh*-expressing cells is reduced in *Wnt7a*<sup>-/-</sup> mice, which indicates that *Wnt7a* is necessary for the maintenance of normal ZPA gene expression.<sup>4</sup> Similar results were obtained in chick embryos. Here, the removal of the dorsal ectoderm and thus *Wnt7a* signal led to a drastic down-regulation of *Shh* expression in the ZPA.<sup>5</sup> In mice (and probably also in humans), the reduction of *Shh* (*SHH*) expression is the likely explanation for the variable loss of posterior skeletal elements—that is, ulna/fibula and digit 5. Interestingly, this phenotype was observed only with the A109T mutation, which, according to our functional assay, results in a relatively mild loss of WNT7A function. Thus, the homozygous null allele in mice corresponds phenotypically to a partial loss of function in humans. In contrast, the R292C mutation is an almost-complete loss-of-function mutation. The observed truncations seen in family 1 can be interpreted as the result of a severe down-regulation of SHH that led, in turn, to a reduction of FGF signaling from the AER, since all three signaling centers have been shown to be mutually dependent. Inactivation of *Wnt7a* in the mouse does indeed result in reduced FGF expression, an effect that is likely to exacerbate the phenotype. A strong reduction in AER signaling, either by surgical removal of the AER in the chick or by inactivation of compound mutations in *Fgf4* and *Fgf8* in the mouse, results in the termination of limb growth by a reduction in proliferation and an increase in apoptosis that gives rise to limb truncations.<sup>3</sup> In mice as well as in humans, mutations that interfere with AER maintenance result in the split-hand, split-foot, or ectrodactyly phenotype.<sup>6</sup> Ectrodactyly was observed in two affected individuals, one individual from each study family. Thus, the loss of WNT7A function has a more severe effect in humans than in mice. The mild effects (hypoplasia of nails) are due to a loss of dorsal structures that are directly determined by WNT7A via LMX1. The more-severe effects (e.g., aplasia of ulnar ray and truncations) are likely to be due to a gradual collapse of the other two signaling centers that control limb growth: the ZPA and the AER. This results in severe truncations that are similar to those observed for *Shh* and FGF inactivation. Furthermore, this species difference may reflect a greater importance of WNT7A in control of limb length in humans compared with mice, through more prolonged support of the ZPA and the AER.

Our studies have further defined the role of WNT7A in human development, have emphasized the interdependence of the morphogenic signaling systems involved in limb formation, and have shown a number of species differences between human and mouse. The phenotypes and expression-pattern data we describe illustrate the importance of WNT7A in dorsoventral as well as proximal-distal limb-axis growth and development.

## Acknowledgments

We thank the families for their help with this project. C.G.W., E.R., K.S., S. Scott, and J.B. were or are supported by the Wellcome Trust. S.M. and P.S. are supported by the Deutsche Forschungsgemeinschaft. R.S. was supported by the Birth Defects Foundation, and C.T. was supported by The Royal Society.

## Web Resources

The URLs for data presented herein are as follows:

BLAST, <http://www.ncbi.nlm.nih.gov/BLAST/>  
Human Genome Browser, <http://genome.ucsc.edu/cgi-bin/hgGateway>

Online Mendelian Inheritance in Man (OMIM), <http://www.ncbi.nlm.nih.gov/Omim/> (for WNT7A phenotypes Al-Awadi/Raas-Rothschild syndrome, Schinzel phocomelia syndrome, limb/pelvis-hypoplasia/aplasia syndrome, and Fuhrmann syndrome)  
Primer3, [http://frodo.wi.mit.edu/cgi-bin/primer3/primer3\\_www.cgi](http://frodo.wi.mit.edu/cgi-bin/primer3/primer3_www.cgi)

Wnt Web site, <http://www.stanford.edu/~rnusse/wntwindow.html>

## References

1. Niswander L (2003) Pattern formation: old models out on a limb. *Nat Rev Genet* 4:133–143
2. Niswander L, Jeffrey S, Martin GR, Tickle C (1994) A positive feedback loop coordinates growth and patterning in the vertebrate limb. *Nature* 371:609–612
3. Sun X, Mariani FV, Martin GR (2002) Functions of FGF signalling from the apical ectodermal ridge in limb development. *Nature* 418:501–508
4. Parr BA, McMahon AP (1995) Dorsalizing signal *Wnt-7a* required for normal polarity of D-V and A-P axes of mouse limb. *Nature* 374:350–353
5. Yang Y, Niswander L (1995) Interaction between the signaling molecules WNT7a and SHH during vertebrate limb development: dorsal signals regulate anteroposterior patterning. *Cell* 80:939–947
6. Kornak U, Mundlos S (2003) Genetic disorders of the skeleton: a developmental approach. *Am J Hum Genet* 73:447–474
7. Tickle C (2004) The contribution of chicken embryology to the understanding of vertebrate limb development. *Mech Dev* 121:1019–1029
8. Riddle RD, Ensini M, Nelson C, Tsuchida T, Jessell TM, Tabin C (1995) Induction of the LIM homeobox gene *Lmx1* by WNT7a establishes dorsoventral pattern in the vertebrate limb. *Cell* 83:631–640
9. Dreyer SD, Zhou G, Baldini A, Winterpacht A, Zabel B, Cole W, Johnson RL, Lee B (1998) Mutations in LMX1B cause abnormal skeletal patterning and renal dysplasia in nail patella syndrome. *Nat Genet* 19:47–50
10. Loomis CA, Harris E, Michaud J, Wurst W, Hanks M, Joyner AL (1996) The mouse *Engrailed-1* gene and ventral limb patterning. *Nature* 382:360–363
11. Morgan BA, Fekete DM (1996) Manipulating gene expression with replication-competent retroviruses. *Methods Cell Biol* 51:185–218
12. Logan M, Tabin C (1998) Targeted gene misexpression in chick limb buds using avian replication-competent retroviruses. *Methods* 14:407–420

13. Seemann P, Schwappacher R, Kjaer KW, Krakow D, Lehmann K, Dawson K, Stricker S, Pohl J, Ploger F, Staub E, Nickel J, Sebald W, Knaus P, Mundlos S (2005) Activating and deactivating mutations in the receptor interaction site of GDF5 cause symphalangism or brachydactyly type A2. *J Clin Invest* 115:2373–2381
14. Kumar D, Duggan MB, Mueller RF, Karbani G (1997) Familial aplasia/hypoplasia of pelvis, femur, fibula, and ulna with abnormal digits in an inbred Pakistani Muslim family: a possible new autosomal recessive disorder with overlapping manifestations of the syndromes of Fuhrmann, Al-Awadi, and Raas-Rothschild. *Am J Med Genet* 70:107–113
15. Woods CG, Valente EM, Bond J, Roberts E (2004) A new method for autozygosity mapping using single nucleotide polymorphisms (SNPs) and ExcludeAR. *J Med Genet* 41:e101
16. Tufan AC, Tuan RS (2001) Wnt regulation of limb mesenchymal chondrogenesis is accompanied by altered N-cadherin-related functions. *FASEB J* 15:1436–1438
17. Stott NS, Jiang TX, Chuong CM (1999) Successive formative stages of precartilaginous mesenchymal condensations in vitro: modulation of cell adhesion by Wnt-7A and BMP-2. *J Cell Physiol* 180:314–324
18. Daumer KM, Tufan AC, Tuan RS (2004) Long-term in vitro analysis of limb cartilage development: involvement of Wnt signaling. *J Cell Biochem* 93:526–541
19. Kengaku M, Capdevila J, Rodriguez-Esteban C, De La Pena J, Johnson RL, Belmonte JC, Tabin CJ (1998) Distinct WNT pathways regulating AER formation and dorsoventral polarity in the chick limb bud. *Science* 280:1274–1277
20. Vogel A, Rodriguez C, Warnken W, Izpisua Belmonte JC (1995) Dorsal cell fate specified by chick Lmx1 during vertebrate limb development. *Nature* 378:716–720
21. Parr BA, Avery EJ, Cygan JA, McMahon AP (1998) The classical mouse mutant postaxial hemimelia results from a mutation in the Wnt 7a gene. *Dev Biol* 202:228–234
22. Chiang C, Litingtung Y, Lee E, Young KE, Corden JL, Westphal H, Beachy PA (1996) Cyclopia and defective axial patterning in mice lacking Sonic hedgehog gene function. *Nature* 383:407–413
23. Niedermaier M, Schwabe GC, Fees S, Helmrich A, Brieske N, Seemann P, Hecht J, Seitz V, Stricker S, Leschik G, Schrock E, Selby PB, Mundlos S (2005) An inversion involving the mouse Shh locus results in brachydactyly through dysregulation of Shh expression. *J Clin Invest* 115:900–909